Isomeric cross sections of fast-neutron-induced reactions on ^{197}Au

M. Avrigeanu and V. Avrigeanu*
Horia Hulubei National Institute for Physics and Nuclear Engineering, P.O. Box MG-6, 077125 Bucharest-Magurele, Romania

M. Diakaki and R. Vlastou
Department of Physics, National Technical University of Athens, Greece
(Received 21 November 2011; revised manuscript received 16 March 2012; published 26 April 2012)

Recent accurate data obtained for the isomeric cross section of the ^{197}Au$(n, 2n)$ reaction provide a valuable opportunity to consider the question of the effective moment of inertia of the nucleus within a local consistent model analysis of all available reaction data for the ^{197}Au target nucleus. Thus, a definite proof of a moment of inertia equal to that of the rigid-body has been obtained for the ^{196}Au nucleus, while indications infer about half the rigid-body for ^{194}Ir.

DOI: 10.1103/PhysRevC.85.044618 PACS number(s): 24.10.−i, 24.60.Dr, 25.40.−h, 27.80.+w

I. INTRODUCTION

The cross sections for nuclear reactions induced by neutrons below 20 MeV are generally considered to be reasonably well known despite many reactions for which the data are too conflicting or incomplete to make possible validation of different model calculations. This is why there is still a lot of interest in the model constraints that are responsible for calculation variance (i) at incident energies below 20 MeV, where the statistical model (SM) calculations are most sensitive to parameters related to residual nuclei and emitted particles, and (ii) above 20–30 MeV, where the pre-equilibrium emission (PE) becomes usually the prevailing process so that the data analysis may better validate the model assumptions.

Among the former SM parameters some of the most important concern the nuclear level density and its Gaussian spin distribution with the dispersion σ determined by the nuclear moment of inertia. Actually, the moment of inertia I plays a basic role within both nuclear reaction and spectroscopic studies, with different features pointed out within each of these fields. Therefore, a brief going over might be worthwhile.

The spin cutoff parameter σ^2 is implicit in the Bethe formula [1] based on the Fermi gas (FG) model, assuming equally spaced single-particle states and no collective levels, while it was related by Bloch [2] to the rotations of the whole nucleus as a rigid body. Ericson [3] expressed σ, in terms of I and the nuclear temperature t, as $\sigma^2 = It/\hbar^2$. At the same time, the rigid-body value I_r was noted as a limit at high excitation, where the nucleus can be described as an ordinary FG, while a constant temperature was found suitable at low excitation, similar to a melting system. Nevertheless I values reduced by $\leqslant$30%, due to pairing interactions, were found with an uncertainty still of the same order as the expected effect [3].

Huizenga and Vandenbosch [4] discussed thoroughly the dependence of the isomeric cross-section ratios on the spin distribution of both the compound and the residual nuclei, and consequently the σ values that can be provided by their SM analysis within reactions for which compound nucleus (CN) formation predominates. The importance of the competitive γ-ray emission that was not considered by former SM analyses was pointed out by Grover [5], including an uncertainty between ∼0.1 and ∼1.6 for the ratio I/I_r reported by various authors until then. Moreover, Grover gave a first comment [6] on the difference between the moment of inertia that describes the spin dependence of the level density and an "effective" moment of inertia which is defined by the energies of the lowest excited level at a given spin J of the nucleus (the yrast levels [7]). It was thus emphasized that, while the former is related to the FG of noninteracting particles, the latter is consistent with the opposite shell model calculations corresponding roughly to $I/I_r \sim 0.5$. The shell structure may also account for values $I < I_r$, for nuclei away from closed shells, and for the opposed case, for nuclei near closed shells [7].

While mainly constant σ^2 values were related formerly to a constant-temperature (CT) level density formula, Hilmann and Grover [8] performed shell model combinatorial calculations using the BCS theory for pairing forces and found definite energy and spin dependencies of I. Gilat [9] also found by means of analytical approximation of shell model calculations that the use of the I_r can reproduce only the gross trend of σ with mass number A, averaged over the shell effects. Behkami and Huizenga [10] found in a similar way that σ^2 values, expressed as a sum of independent contributions of σ_n^2 and σ_p^2, depend on the structure of single-particle levels which may completely reverse the importance of the roles of neutrons and protons. Furthermore, Huizenga *et al.* [11] showed that values of σ^2 for doubly even nuclei with $20 \leqslant A \leqslant 209$ at a fixed excitation energy $E^* = 7$ MeV do not increase smoothly with A but show structure reflecting the angular momenta of the shell model orbitals near the Fermi energy. This structure was proved soon after that by Canty *et al.* [12], through comparison of realistic shell model calculations with FG model level density, to be washing out with the increase of E^* up to 50–60 MeV. A particular case was pointed out at the same time by Joly *et al.* [13] by analysis of γ-ray strength functions deduced from neutron capture between 0.5 and 3 MeV, namely, I_r values for near closed-shell nuclei ^{104}Rh and ^{198}Au and half of I_r for the deformed nucleus ^{170}Tm.

*Vlad.Avrigeanu@nipne.ro

The knowledge about the level density spin cutoff factor σ, available until the beginning of the 1970s, from isomer ratio and angular distribution measurements was reviewed and completed through the latter way by Lu *et al.* [14], taking into account its energy dependence and discussing the motivation of finding various I/I_r values. Taking also the advantage of the higher angular momenta brought by heavier incident α particles, they provided evidence for the full I_r. The smaller I values reported previously were considered to be due to incorrect assumptions and approximations. The same motivation was found by Hille *et al.* [15] also by analysis of angular distribution, for 50% decrease of a former established I/I_r value. On the other hand, a new and direct determination of the spin cutoff factor was introduced in the beginning of the 1980s by Weigmann *et al.* [16] by comparison of both neutron and proton resonance data for the same compound nucleus ^{41}K, with the corresponding result $I/I_r \sim 1.00 \pm 0.18$.

A significant development of the theoretical approaches came out in the 1990s. Thus, a proper description of the energy-dependent spin cutoff factor deduced from both the spin distribution of the low-lying levels and the resonance data proved the consistency of the phenomenological generalized superfluid model, taking into account the phase transition from the superfluid state to the normal state at a critical temperature lower than $\Delta_0 = 12/\sqrt{A}$ [17]. Actually, according to this phase transition, the authors of a reviewed resonance data analysis [18] themselves considered the result of a half of I_r surprising. Moreover, a microscopic approach [19] led to a moment of inertia that is about half of the I_r value at lower excitation energy, due to the pairing correlations, and increases by ~15% at higher excitation. However, a dramatic increase in the moment of inertia up to the I_r value was shown to be associated with the breaking of nucleon pairs for temperatures of 1.0–1.5 MeV, within shell model Monte Carlo (SMMC) calculations [20] as well as, later on, in a simplified spin cutoff model [21]. Further developments made possible conversion of the SMMC values of σ^2 to an energy-dependent I that is at low energies significantly smaller than the I_r value due to the pairing correlations [22].

However, the moment of inertia assessment based on the spin distribution analysis at low excitation is related to the spectroscopic information that has been available up to a few 100 keV above the yrast line, beyond the low-lying levels and resonance data with spins usually $\leqslant 5\hbar$ (e.g., Ref. [23]). Sorensen [24] reviewed at length that, while the moment of inertia given by the measured energies of yrast levels in a number of rare-earth nuclei is two to three times smaller than the I_r values due to the pairing correlations, it increases smoothly with the spin increasing, for low angular momenta, until suddenly it rises at about spin 14–16 to I_r. The backbending, i.e., anomalous behavior of the moment of inertia at high spin in nuclear rotational bands of medium and heavy nuclei, where I rises faster than J, was related to a phase transition to vanished pairing correlations that takes place over several J units. Moreover, Bohr and Mottelson [25] pointed out the differences between the "dynamical" effective moment of inertia, defined by the "envelope" of the yrast bands, and those defined by individual bands, with respect to the I_r value, and the fact that the available resolved band spectra give information on the rotation of the nucleus in its superfluid phase. Large variations of I were also showed to be caused by shape change, collapse of pairing correlation or alignment of particles in transitional nuclei [26] like these within present work. More recently, I values at high spin that may be substantially smaller than I_r values as if the nucleus was superfluid, while it was already in the normal state, were attributed to shell effects [27]. However, for the shape transitional nuclei, or almost spherical nuclei, the I values may increase with spin much faster [28].

In the meantime, a value of $I/I_r = 0.75 \pm 0.06$ at the neutron binding energy for the nucleus ^{51}V [29], obtained by the direct method of Weigmann *et al.* [16], was later considered in two different ways. Thus, a variable moment of inertia was adopted between the 0.5 and 0.75 values of I/I_r, for the excitation energies from the nucleus ground state (g.s.) to the nucleon binding energy, and then to 1 around $E^* = 15$ MeV [29]. It was next involved within consistent analyses of the isomeric cross-section ratio [30–36] with good results. However, it was also found that even the largest change between the 0.5 and 1 values of I/I_r may be still of the same magnitude with the uncertainties associated with the decay schemes and measured-data spread, so that a definitive conclusion on this point was precluded [30]. On the other hand, the I/I_r value of 0.75 for $A \sim 50$ [29], taken into account in the whole E^* range, and values of 0.15–0.30 found in analyses of isomeric cross-section ratios for $A \sim 140$ [37] and $A \sim 200$ [38–41] led the authors of the latest references to the assumption of a mass-dependent effective moment of inertia. Similar calculations for lead isotopes have shown that the isomer population is more readily reproduced using an I value that is half rather than the full I_r [42].

The above review of the knowledge gathering about spin cutoff factor σ^2 may account for the results obtained by level counting at low energy, starting with analyses [43] that assumed only the dependence on A. At later times, a similar but enlarged study [44] found a weak A dependence that could be attributed to a value $I < I_r$ below the excitation energies of 6–8 MeV, while most recent work of these authors [45] gave the spin cutoff factor as a function of both A and E^*, with similar conclusions. Meanwhile, a parallel study but within both FG and CT models, done finally for $20 \leqslant A \leqslant 110$ [46], indicated that I at energies of a few MeV is slightly less than I_r. More recently, Koning *et al.* [47] gave both a closed form of the discrete spin cutoff σ_d^2 and a suggestive view of the difference between this value and the FG one at the neutron binding energy versus A (Fig. 5 of Ref. [47]). A linear interpolation is adopted between the two values [47,48].

A thorough way of using the data available in the whole excitation range in analysis of the isomeric cross sections was initiated by Chadwick and Young [49], with a spin cutoff factor interpolated linearly between the σ^2 value determined from the spin distribution of observed low-lying discrete levels and the FG value adopted within the related E^* range. They also took into account 14^+, 15^+, and 16^+ discrete levels embedded within the continuum of statistically described levels, which decay into the isomeric 16^+ state of ^{178}Hf, to describe its population. An increase of 30–40% for this population cross section was thus obtained, while these authors considered that the existence of such undetected bands that decay fully into the isomeric state is physically unlikely. Soon after, they proved [50] that better results for this yet quite particular case [51] are obtained provided that the same spin distribution after PE and equilibrium decay is not assumed. While the PE spin distribution was discussed early on by Feshbach *et al.* [52] and further detailed by Fu [53], its basic role for a proper analysis of the isomeric cross-section ratios was first proved by Bogila *et al.* [54] for proton incident energies above 25 MeV. A decade later the Los Alamos group [55] proved that, taking properly into account the PE spin distribution for neutron inelastic scattering on ^{193}Ir, the $11/2^-$ isomer production cross section is reduced by 50% at 14 MeV. Moreover, it was also shown that, while the production cross section of a high-spin isomer through a $(n, 2n)$ reaction would be reduced by including the real PE spin distribution, the same effect may be obtained using only the CN spin distribution with a significantly reduced σ^2 value [56]. These authors noted that the above-mentioned rather strong decrease of the ratio I_r/I to 0.15–0.20 [39] was artificial and resulted from the use of an improper PE spin distribution, i.e., the CN one. Further calculations [57] using PE spin distribution do not indicate a need for the value $I < I_r$.

The so different statements [38–42,55–59] for the level density spin cutoff obtained from isomer-ratio measurements in the transitional region from well-deformed to spherical nuclei near the $Z = 82$ shell closure and the new accurate data obtained for the reaction ^{197}Au$(n, 2n)$ [59] motivate this analysis. The reaction models involved and the consistent parameter set adopted to avoid compensation effects in the case of improperly adjusted parameters are discussed in Sec. II. The calculated results are compared in a unitary way with the available data for all reaction channels in Sec. III. Questions still existing are discussed in Sec. IV, and conclusions are given in Sec. V. Preliminary results are described elsewhere [60].

II. NUCLEAR MODELS AND PARAMETERS

To avoid the usual question marks associated with the model calculations which combine PE with equilibrium decay of the remaining compound nucleus, we have analyzed the activation cross sections of the ^{197}Au target nucleus using a consistent local parameter set, established by distinct analyses of various independent data. An updated version of the STAPRE-H95 code [61,62] has also been used, including a generalized geometry-dependent hybrid (GDH) model [63] for PE processes, which takes into account the angular-momentum conservation [64] and α-particle emission [65] with a preformation probability φ [66] that is assumed to have a 0.25 value [67]. The same optical model potential (OMP) and nuclear level density parameters were used, beyond the OM and SM frameworks, for the calculation of the PE model intranuclear transition rates and single-particle level (s.p.l.) densities at the Fermi level [63,68,69], respectively.

The comparison of various measured data and calculation results, including their sensitivity to model approaches and parameters, has concerned all activation channels for which there are measured data. Thus, the use of model parameters that may be improperly adjusted, to take into account properties peculiar to specific nuclei in the decay cascade, was avoided. The unitary character of the model analysis is thus also ensured.

The nucleon optical potential of Koning and Delaroche [70] was found to describe adequately [60] the Reference Input Parameter Library (RIPL-3) recommendations for the low-energy neutron scattering properties [48] as well as the recent neutron total cross sections [71]. Actually we used the neutron transmission coefficients obtained within the code TALYS [72] by using RIPL 1464 potential segment. The same TALYS calculation has been used to obtain the fraction of the neutron reaction cross section corresponding to the collective inelastic scattering cross sections. Typical ratios of the direct inelastic scattering to the total reaction cross sections in the incident energy range from 4 to 40 MeV decrease from $\sim$20% to 3%, being used for the corresponding decrease of the latter within the rest of the reaction cross-section calculations.

For calculation of the α-particle transmission coefficients, we have used the optical potential established previously [73] for emitted α-particles and supported recently by semimicroscopic analysis for $A \sim 90$ nuclei [74].

The modified energy-dependent Breit-Wigner (EDBW) model [75,76] was used for the electric dipole γ-ray strength functions $f_{E1}(E_\gamma)$ requested for calculation of the γ-ray transmission coefficients. The systematic EDBW-model correction factor F_{SR} has been chosen to provide $f_{E1}(E_\gamma)$ values close to the related experimental data and former calculations (Refs. [77,78]). At the same time we used the γ-ray strength function f_{M1} parameters of Ref. [78] as well as global estimations [79] of the γ-ray strength functions for the other multipoles $\lambda \leqslant 3$. The corresponding strength functions have finally been checked within the calculations of capture cross sections of ^{197}Au nucleus in the neutron energy range from keV to $\sim$8 MeV [60], using also the OMP and nuclear level density parameters described below.

The nuclear level densities were derived on the basis of the backshifted Fermi gas (BSFG) formula [80], for the excitation energies below the neutron-binding energy, with the parameters a and Δ obtained by fit of recent experimental low-lying discrete levels [81] and s-wave nucleon resonance spacings D_0 [48]. Above the neutron binding we took into account the washing out of shell effects [82,83] using the method of Koning and Chadwick [84] for fixing the appropriate shell correction energy. To have a smooth connection we chose a transition range from the BSFG formula description to the higher energy approach, between the neutron binding energy and the excitation energy of 15 MeV. Concerning the level density spin distribution, we first used the above-mentioned variable ratio I/I_r varying among values of 0.5 for ground states, 0.75 at the neutron binding energy, and 1 around the excitation energy of 15 MeV [29]. The results below proved however the need to consider a constant ratio I/I_r, equal to either 1 or 0.5. Therefore we did the fit of low-lying discrete levels [81] and s-wave nucleon resonance spacings D_0 also for these constant I/I_r values in the range $187 < A < 206$. The three sets of the a parameter values obtained in this way are shown elsewhere [60] while the values for the case $I/I_r = 1$ are given in Table I. For the nuclei without resonance data we applied the smooth-curve method [79] by using average a

TABLE I. Low-lying level number N_d up to excitation energy E_d^* [81] used in cross-section calculations and the levels and s-wave neutron-resonance spacings $D_0^{\rm exp}$ in the energy range ΔE above the separation energy S, for the target-nucleus g.s. spin I_0, fitted to obtain the BSFG level density parameter a and g.s. shift Δ, for a spin cutoff factor calculated with the rigid-body value for the nucleus moment of inertia, and reduced radius $r_0 = 1.25$ fm.

Nucleus	N_d	E_d^*	Fitted level and resonance data					a	Δ
			N_d	E_d^*	$S+\frac{\Delta E}{2}$	I_0	$D_0^{\rm exp}$		
		(MeV)		(MeV)	(MeV)		(keV)	(MeV^{-1})	(MeV)
^{190}Ir	26	0.287	59	0.486				20.40	−1.19
^{191}Ir	20	0.686	20	0.686				19.60	−0.63
^{192}Ir	28	0.235	35	0.284	6.198	3/2	0.0025(3)	20.40	−1.31
^{193}Ir	29	0.874	29	0.874				19.46	−0.62
^{194}Ir	36	0.489	36	0.489	6.067	3/2	0.0058(5)	20.00	−1.04
^{193}Pt	32	0.701	32	0.701	6.256	0	0.0314(13)	19.58	−0.79
^{194}Pt	27	1.816	42	2.004				19.00	0.41
^{195}Pt	28	0.695	28	0.695	6.106	0	0.082(10)	18.30	−0.86
^{196}Pt	45	2.013	54	2.093	7.922	1/2	0.018(3)	18.32	0.33
^{197}Pt	23	0.797	27	0.859	5.847	0	0.35(10)	16.65	−0.85
^{193}Au	22	1.284	22	1.284				19.50	−0.05
^{194}Au	12	0.619	4	0.245				20.00	−0.97
^{195}Au	36	1.443	36	1.443				18.80	−0.12
^{196}Au	56	0.598	56	0.598				19.00	−1.17
^{197}Au	14	0.948	14	0.948				17.00	−0.45
^{198}Au	30	0.573	30	0.573	6.515	3/2	0.0155(8)	17.50	−1.13

values, given by the narrow A-range systematics, for the fit of the low-lying discrete levels.

Concerning the particle-hole state density (PSD) that plays the same role for the PE description as the nuclear-level density for SM calculations, a composite formula [69] was used within the GDH model, with no free parameters except for the α-particle state density $g_\alpha = A/10.36$ MeV^{-1} [67]. The PSD's most important correction for the nuclear potential finite-depth was obtained by using the Fermi energy value $F = 37$ MeV [85], while formerly [60] the value $F = 40$ MeV [63] was adopted. A linear energy dependence was adopted for the s.p.l. density g of the PE excited particles, at the same time with the FG model form for the exciton-configuration hole density g_h (Ref. [69] and Refs. therein).

III. MODEL CALCULATION RESULTS

A. The (n, xn) reactions

First we should note the good agreement of the calculated cross sections for the ^{197}Au$(n,2n)^{196}$Au reaction with the measured data (Fig. 1) especially concerning the most recent and accurate experiment [59] as well as the ones within the last decade [86]. However, the sensitivity of these calculations to the abovementioned three options for the nuclear moment of inertia is so low that no conclusion is possible. However, the larger spreading of data shown in Fig. 1(a) around the incident energy of 14 MeV, where our calculated values match the lower limit of the most recent data [86], proves the usefulness of additional accurate measurements even at these energies. The same applies to the evaluated data [88] from ∼14 to 30 MeV, while our calculations, however, describe well the recent data [Fig. 1(c)]. Nevertheless, the large error bars of the data measured above 30 MeV put the support of model calculations under question. Hence the need for new accurate measurements.

The comparison of the calculated and experimental cross sections for the population of the high-spin second isomeric state through the $(n,2n)$ reaction is quite a different case. This isomeric state is the 55th excited state of the ^{196}Au residual nucleus at the top of the discrete levels taken into account in the SM calculations. Thus its population comes from the side feeding and continuum decay, so that it is fully determined by the nuclear level density and γ-ray strength functions. While the latter quantities were found to be suitably considered [60], the model sensitivity to the nuclear moment of inertia assumption shown in Fig. 1(b) is so large that it makes possible a certain conclusion on the real ratio I/I_r. The high accuracy of data recently measured [59,86] leads to a value around 1.

Unfortunately the error bars in the data set available above 20 MeV [Fig. 1(d)] are so large, $\geqslant$50%, that no further assessment can be concluded on either the correct moment of inertia or the key PE model quantities that become most important at these energies (e.g., Refs. [32,33]).

Similar cases of missing data with higher accuracy or better incident energy resolution are shown in Fig. 2 for the $(n,3n)$ and $(n,4n)$ reactions on ^{197}Au. On the basis of the comparison between the measured data and actual model calculations, one may notice the obvious need for improved experimental data that can establish the accuracy of the actual phenomenological models.

B. The (n, p) reaction

A requirement for a unitary reaction model analysis is the similar description of all measured data for various reaction

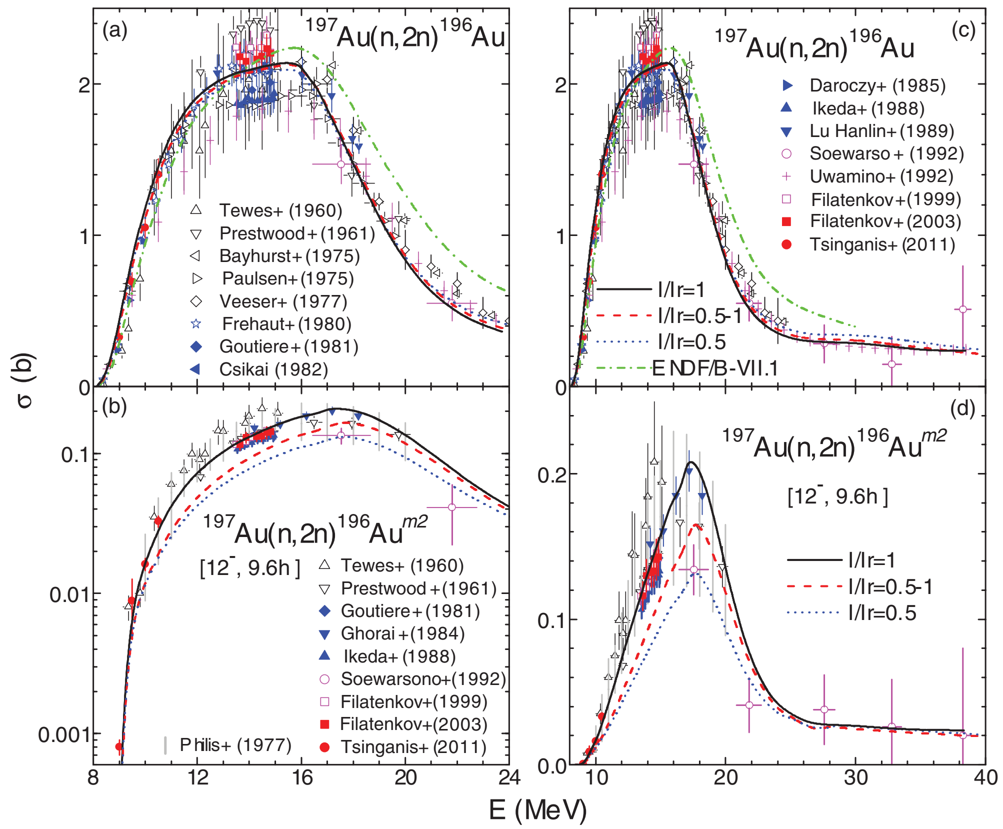

FIG. 1. (Color online) Comparison of experimental [59,86,87], ENDF/B-VII.1 evaluated [88], and calculated cross sections of the reactions (a,c) ^{197}Au$(n,2n)^{196}$Au and (b,d) ^{197}Au$(n,2n)^{196}$Au^{m2} (with the corresponding spin, parity, and lifetime shown between square brackets), for incident energies up to (a,b) 24 MeV and (c,d) 40 MeV, by using the excitation-energy variable ratio I/I_r of the nuclear moment of inertia to its rigid-body value (dashed curve) or the constant ratios 0.5 (dotted) and 1 (solid).

channels, i.e., the (n,p) and (n,α) reactions for the ^{197}Au target nucleus. Moreover, well-known isomeric states are also populated through these reactions, and their study is a challenge for the present conclusions on the nucleus moment of inertia. Regarding the (n,p) reaction, our calculation results describe rather well the most recent experimental data [86] for the population of the ground and isomeric states of the residual nucleus ^{197}Pt as well as the corresponding isomeric ratio (Fig. 3). However the related sensitivity of the ^{197}Au$(n,p)^{197}$Pt^m reaction cross sections is much lower than that of the previous case, due to the lower isomeric state spin and excitation energy, as well as the different decay scheme. Actually this comparison is just pointing out the particular case of the high-spin second isomeric state of the ^{196}Au nucleus.

C. The (n,α) reaction

Similar comments may apply in the case of the (n,α) reaction shown in Fig. 4 but with an unexpected large overestimation of the isomeric cross sections measured at the same time as those for the g.s. population. Actually this isomeric state has uncertain spin (either $10\hbar$ or $11\hbar$), parity, and excitation energy of $190+x$ keV, where $x \leqslant 250$ keV [89]. While the calculated isomeric cross sections are not sensitive to the excitation energy, assumed by us to be 440 keV, the spin value is quite important. We have considered, in agreement with the neighboring similar isotopes, the spin and parity 11^- for this isomeric state. This assumption obviously leads to lower reactions cross sections, the calculated results being still larger than the measured data. The sensitivity of the calculated isomeric cross sections with respect to the moment of inertia in this case is comparable to the experimental errors, but the results corresponding to the ratio $I/I_r = 0.5$ are closer to the measured data.

IV. DISCUSSION

A. Discrete spin cutoff

The results of the present model analysis are validated by the use of a consistent set of model parameters, established through distinct analyses of various independent data, as well as of advanced reaction-model assumptions and formalisms. The current finding of a moment of inertia equal to that of the rigid-body for ^{196}Au is compared in Fig. 5 with other actual

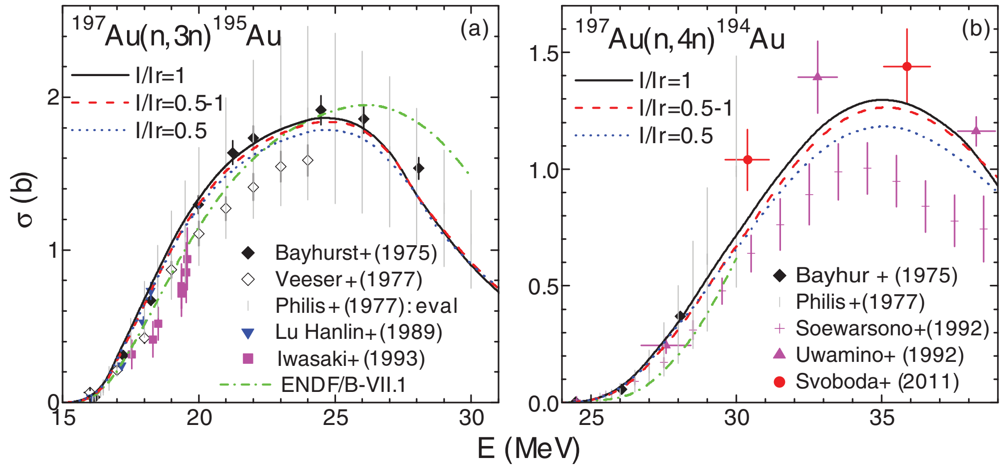

FIG. 2. (Color online) As for Fig. 1, but for (a) the $(n, 3n)$ reaction and (b) the $(n, 4n)$ reaction on ^{197}Au.

formulas of the level density spin cutoff σ^2. These are the usual alternative half rigid-body moment of inertia, the latest energy-dependent parametrization (Eq. (16) of Ref. [45]), and the discrete spin cutoff σ_d^2 [47] for the levels of the nucleus ^{196}Au given in Table I, which is so close to the global value given within the same Ref. [47]. Also shown is the energy-dependent spin cutoff $\sigma^2(E_d^*)$ given by the maximum likelihood estimator, following the discussion in Ref. [90], namely, the ratio of the sum of the $(J_i + 1/2)^2$ term for all discrete levels with $E_i^* < E_d^*$, to twice the number of these levels. This quantity is also shown for the nucleus ^{194}Ir.

The various σ^2 values obtained through distinct methods and systematics shown in Fig. 5 need obviously further investigations beyond the ones briefly reviewed in Sec. I just for an overall picture. The significant differences between various estimations even for the same energy range, e.g., Refs. [45,47], might be argued by the limited excitation energy as well as spin ranges of the low-lying discrete levels available for nuclei in the mass region $A \sim 190$ that were considered within the involved parametrizations.

B. Nuclear moments of inertia for various nuclei

The considerable change found in this work for the I/I_r value from 1 for ^{196}Au to $\leqslant$0.5 for ^{194}Ir may have several sources, especially taking into account that the two nuclei differ one from the other by only a pair of protons. First, one should note the quite distinct mechanism by which they are populated. Thus, for the same neutron incident energy of 15 MeV, the former nucleus is populated by the fully equilibrated secondary-neutron emission following a 17.5% weight for the PE processes in the first reaction stage. The opposite case is that of the corresponding α-particle decay, the residual nucleus ^{194}Ir being populated by $\sim$83% α-particle PE, as is usual for charged-particle evaporation suppressed by the Coulomb barrier in heavy-mass nuclei. This implies that the major contribution to the feeding of the ^{194}Ir metastable state arises from the spin cutoff considered for the PE description, within the partial level densities [69]. Actually the same partial level density formula has also been used [65] for description of the proton PE emission that has an $\sim$88% weight, and the populations of both the ground and isomeric states of the

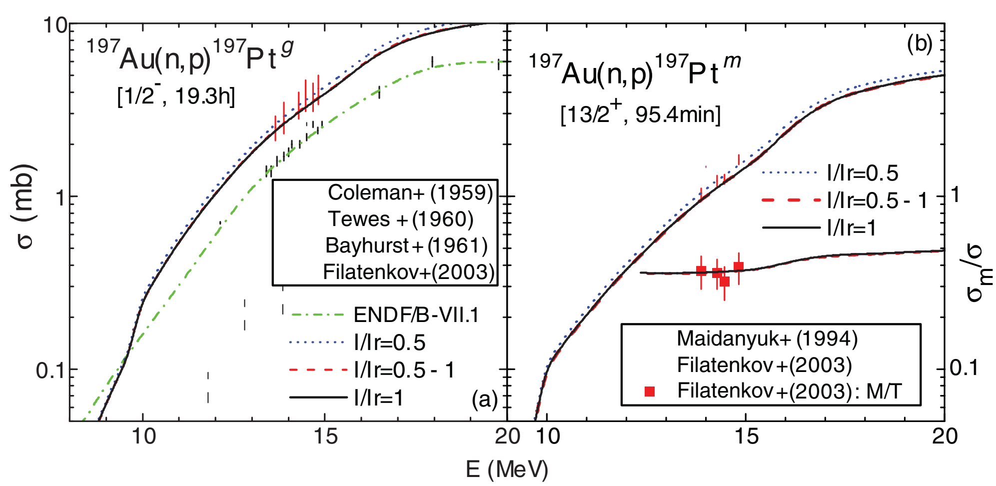

FIG. 3. (Color online) As for Fig. 1, but for the (n, p) reaction and population of (a) the g.s. and (b) the isomeric state of the residual nucleus ^{197}Pt, and (b) the same comparison for the isomeric ratio.

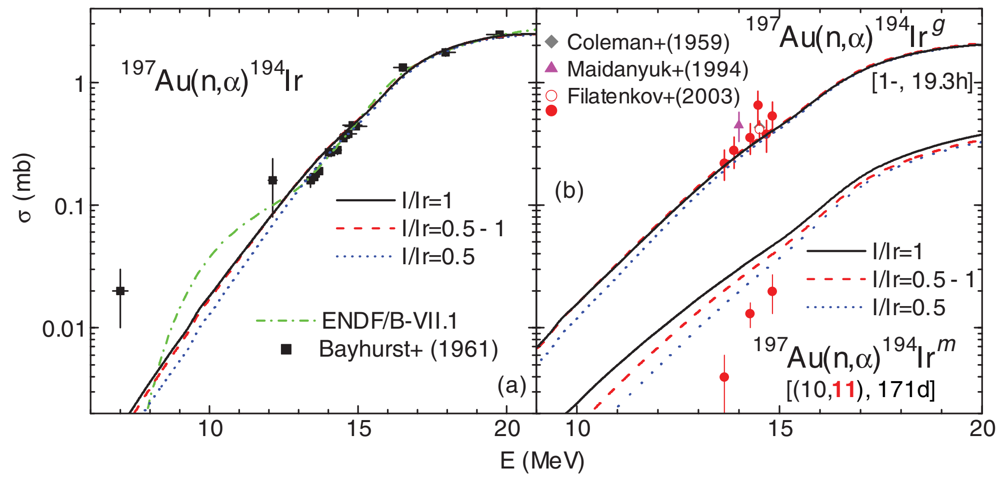

FIG. 4. (Color online) As for Fig. 1, but for (a) (n,α) reaction cross sections for the target nucleus ^{197}Au and (b) population of the g.s and isomeric state of the residual nucleus ^{194}Ir. The actual evaluation data [89] are shown for the spin and parity of the isomeric state while the value 11^- has been used in the calculation (see text for details).

corresponding residual nucleus ^{197}Pt are quite well described (Fig. 3). Therefore we may conclude that the experiment and model agreement for the isomeric cross section of the ^{196}Au nucleus proves the correctness of the spin cutoff corresponding to the rigid-body moment of inertia for the neutron emission at equilibrium, while the same agreement for the ^{197}Pt nucleus indicates the correctness of the implemented nucleon PE spin cutoff. It should be noted, however, that the PE mechanism for α particles [66] is rather different from the usual one for nucleons.

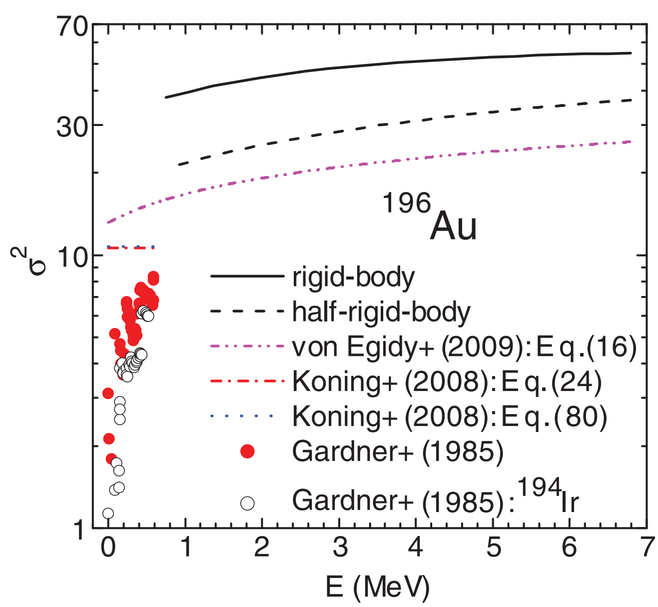

FIG. 5. (Color online) The excitation-energy dependence of the level density spin cutoff for the nucleus ^{196}Au corresponding to rigid-body (solid curve) and half rigid-body (dashed) moments of inertia, the energy-dependent parametrization of Ref. [45] (dash-dot-dotted), the discrete spin cutoff (dash-dotted) and its global value (dotted) of Ref. [47], and given by the maximum likelihood estimator [90] (solid circles). The latest quantity is also shown for the nucleus ^{194}Ir (open circles).

Second, preliminary cranking-formula calculations of the moment of inertia for the ground states of ^{194}Ir and ^{196}Au nuclei [91] have given a ratio of 0.73 between them. This result is in agreement with the discrete spin cutoff σ_d^2 values [90] of the nuclei ^{196}Au and ^{194}Ir (Fig. 5). Despite the need for further cranking calculation that should take into account the pairing vanishing, there is thus a hint to a rather significant difference between the moments of inertia of the two nuclei.

Third, there is a point at which one should look before a final search for the isomeric ratio of ^{194}Ir by studying the ^{197}Au$(n,\alpha)^{194}$Ir reaction. It is related to the question of different α-particle OMP parameters in the incident and outgoing channels, with consequences for the present case discussed elsewhere [60]. Because this OMP has a key role for the calculation of both the α-particle transmission coefficients and the GDH intranuclear transition rates, we shall look first for the answer to this difference. The advantage of the recent global consistent description of α-particle OMP in the incident channel [34] will be taken in this respect. Therefore, for the time being we remain with the only hint of a value less than or equal to the half rigid-body moment of inertia for the ^{194}Ir nucleus populated through the (n,α) reaction. A comparison with the exact corresponding value $I/I_r = 0.31 \pm 0.02$ [41] is not yet possible because the isomeric state spin and the α-particle OMP used in Ref. [41] are not known.

A point that should be made clear for any case concerns the eventual importance of the equipartition of the parities considered as usual for the level densities involved in the present work. Among various approaches for this question we have considered the simpler but faster one of Pichon [92]. This model makes use of an asymmetry ratio $A(E^*)$ between the difference of the number of levels with the parities +1 and −1, respectively, and their sum. Moreover, it assumes that $A(E^*)$ goes to 0 linearly, starting from the energy of the first excited level with the parity opposite to the ground-state parity. This energy is 0.085 and 0.147 MeV, respectively, for ^{196}Au

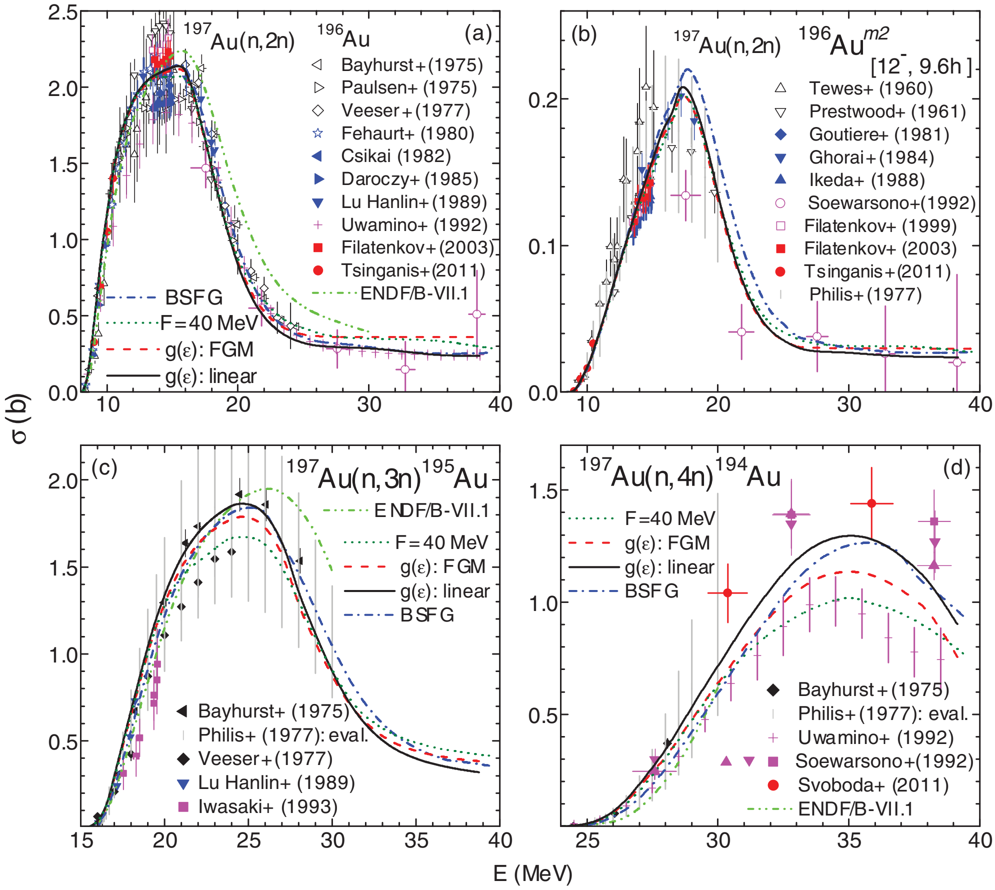

FIG. 6. (Color online) Comparison of experimental [87], ENDF/B-VII.1 evaluated [88], and calculated (n, xn) reaction cross sections for the target nucleus ^{197}Au, by using the model assumptions and parameters given in the text (solid curves) and the alternative replacement of either the Fermi energy value $F = 40$ MeV (dotted) or the FG energy dependence of the s.p.l. density g of PE excited particles (dashed), or use of only the BSFG formula for the nuclear level density (dash-dotted).

and ^{194}Ir. Moreover, using the number of levels with the two parities up to limits of the low-lying levels given in Table I, we found that the equipartition of parities is achieved in the two nuclei at 0.94 and 0.97 MeV, respectively. Even by taking into account roughly this outcome of a so straightforward approach, it results that the parity-equipartition assumption plays no role in the present analysis.

C. Pre-equilibrium emission model assumptions

Finally, while the present local analysis has been able to provide a suitable description of most of the available data, Fig. 6 shows that PE model assumptions could be not responsible for any real effect on the calculated isomeric cross sections especially below incident energy of ∼17 MeV. However, these model constrains could be better proved by analysis of the (n, xn) reaction data above 20–30 MeV. Nevertheless, it is obvious that improved experimental data are needed to establish, e.g., the correctness of the $(n, 3n)$ and $(n, 4n)$ reaction excitation function changes owing to different values of the Fermi energy. These changes follow the start of PE contributions due to a higher angular momentum, which happens when the corresponding local density Fermi energies (e.g., Fig. 4 of Ref [31]) become larger than the average excitation energy of exciton holes, within the PSD nuclear potential finite-depth correction.

The cross-section variations shown in Fig. 6 are related also to either the use of the FG model or a linear energy dependence of the s.p.l. density of excited particles within the PE exciton configurations. A description of the nuclear level density by means of the BSFG formula at any excitation energy leads to eventual changes of the excitation functions at larger energies. However only a few data sets, with large uncertainties, are available within this energy range. Therefore further measurements to be performed consistently at large-scale facilities such as SPIRAL-2 [93] and n_TOF [94], for incident energies from threshold up to 40 as well as 100 MeV, may definitely contribute to the increase of the predictability power of actual phenomenological models. Currently no related microscopic models of a similar strength are available.

V. CONCLUSIONS

Questions of consistent model analysis of all available fast-neutron reaction data for the ^{197}Au target nucleus have been discussed within a local approach, using model parameters established or validated by independent analyses of various experimental data other than the activation cross sections that are the object of this work. It has thus been possible to describe most of these data in a unitary way, while this work has shown a definite proof of a moment of inertia equal to that of the rigid-body for ^{196}Au, by analyzing the population of its high–spin second isomeric state through the $(n,2n)$ reaction.

A still open question concerns, however, a present hint of a value less than or equal to the half rigid-body moment of inertia for the ^{194}Ir nucleus populated through the (n,α) reaction. Further work within the cranking formula would be beneficial to account for the large change of the I/I_r value from ^{196}Au to ^{194}Ir; further work on the question of different α-particle OMP parameters in the incident and outgoing channels would also be beneficial. Nevertheless, the usefulness of further measurements to be performed at large-scale facilities, for incident energies up to 40 as well as 100 MeV, is obvious to establish, e.g., the correctness of the $(n,3n)$ and $(n,4n)$ reaction excitation-function changes owing to different PE model assumptions.

ACKNOWLEDGMENTS

We thank Mihai Mirea for useful discussions. This work was partly supported by a grant from the Romanian National Authority for Scientific Research, CNCS-UEFISCDI, Project No. PN-II-ID-PCE-2011-3-0450.

[1] H. A. Bethe, Rev. Mod. Phys. **9**, 69 (1937).
[2] C. Bloch, Phys. Rev. **93**, 1094 (1954).
[3] T. Ericson, Nucl. Phys. **11**, 481 (1959).
[4] J. R. Huizenga and R. Vandenbosch, Phys. Rev. **120**, 1305 (1960); R. Vandenbosch and J. R. Huizenga, *ibid.* **120**, 1313 (1960).
[5] J. R. Grover, Phys. Rev. **123**, 267 (1961).
[6] J. R. Grover, Phys. Rev. **127**, 2142 (1962).
[7] J. R. Grover, Phys. Rev. **157**, 832 (1967).
[8] M. Hilmann and J. R. Grover, Phys. Rev. **185**, 1303 (1969).
[9] J. Gilat, Phys. Rev. C **1**, 1432 (1970).
[10] A. N. Behkami and J. R. Huizenga, Nucl. Phys. A **217**, 78 (1973).
[11] J. R. Huizenga, A. N. Behkami, R. W. Atcher, J. S. Sventek, H. C. Britt, and H. Freiesleben, Nucl. Phys. A **223**, 589 (1974).
[12] M. J. Canty, P. A. Gottschalk, and F. Pühlhover, Nucl. Phys. A **317**, 495 (1979).
[13] S. Joly, D. M. Drake, and L. Nilsson, Phys. Rev. C **20**, 2072 (1979).
[14] C. C. Lu, L. C. Vaz, and J. R. Huizenga, Nucl. Phys. A **197**, 321 (1972).
[15] P. Hille, P. Sperr, M. Hille, K. Rudolph, W. Assmann, and D. Evers, Nucl. Phys. A **232**, 157 (1974).
[16] H. Weigmann, C. Wagemans, A. Emsallem, and M. Asghar, Nucl. Phys. A **368**, 117 (1981).
[17] A. V. Ignatyuk, J. L. Weil, S. Raman, and S. Kahane, Phys. Rev. C **47**, 1504 (1993).
[18] S. F. Mughabghab and C. Dunford, Phys. Rev. Lett. **81**, 4083 (1998).
[19] B. K. Agrawal, S. K. Samaddar, A. Ansari, and J. N. De, Phys. Rev. C **59**, 3109 (1999).
[20] D. J. Dean, S. E. Koonin, K. Langanke, P. B. Radha, and Y. Alhassid, Phys. Rev. Lett. **74**, 2909 (1995); K. Langanke, D. J. Dean, S. E. Koonin, and P. B. Radha, Nucl. Phys. A **613**, 253 (1997).
[21] Y. Alhassid, G. F. Bertsch, L. Fang, and S. Liu, Phys. Rev. C **72**, 064326 (2005).
[22] Y. Alhassid, S. Liu, and H. Nakada, Phys. Rev. Lett. **99**, 162504 (2007).
[23] H. A. Weidenmüller and G. E. Mitchell, Rev. Mod. Phys. **81**, 539 (2009).
[24] R. A. Sorensen, Rev. Mod. Phys. **45**, 353 (1973).
[25] A. Bohr and B. R. Mottelson, Phys. Scr. **24**, 71 (1981).
[26] V. Martin and J. L. Egido, Phys. Rev. C **51**, 3084 (1995).
[27] M. A. Deleplanque, S. Frauendorf, V. V. Pashkevich, S. Y. Chu, and A. Unzhakova, Phys. Rev. C **69**, 044309 (2004).
[28] J. B. Gupta and J. H. Hamilton, Phys. Rev. C **83**, 064312 (2011).
[29] V. Avrigeanu, T. Glodariu, A. J. M. Plompen, and H. Weigmann, J. Nucl. Sci. Technol. Suppl. **2**, 746 (2002).
[30] V. Semkova, V. Avrigeanu, T. Glodariu, A. J. Koning, A. J. M. Plompen, D. L. Smith, and S. Sudar, Nucl. Phys. A **730**, 255 (2004).
[31] P. Reimer, V. Avrigeanu, S. V. Chuvaev, A. A. Filatenkov, T. Glodariu, A. Koning, A. J. M. Plompen, S. M. Qaim, D. L. Smith, and H. Weigmann, Phys. Rev. C **71**, 044617 (2005).
[32] V. Avrigeanu, R. Eichin, R. A. Forrest, H. Freiesleben, M. Herman, A. J. Koning, and K. Seidel, Nucl. Phys. A **765**, 1 (2006).
[33] M. Avrigeanu, S. Chuvaev, A. A. Filatenkov, R. A. Forrest, M. Herman, A. J. Koning, A. J. M. Plompen, F. L. Roman, and V. Avrigeanu, Nucl. Phys. A **806**, 15 (2008).
[34] M. Avrigeanu, A. C. Obreja, F. L. Roman, V. Avrigeanu, and W. von Oertzen, At. Data Nucl. Data Tables **95**, 501 (2009); M. Avrigeanu and V. Avrigeanu, Phys. Rev. C **82**, 014606 (2010).
[35] V. Avrigeanu and M. Avrigeanu, Phys. Rev. C **83**, 017601 (2011).
[36] D. Filipescu *et al.*, Phys. Rev. C **83**, 064609 (2011).
[37] K. Hilgers, S. Sudár, and S. M. Qaim, Phys. Rev. C **76**, 064601 (2007).
[38] S. Sudár and S. M. Qaim, Phys. Rev. C **73**, 034613 (2006).
[39] M. Al-Abyad, S. Sudár, M. N. H. Comsan, and S. M. Qaim, Phys. Rev. C **73**, 064608 (2006).
[40] M. S. Uddin, B. Scholten, A. Hermanne, S. Sudár, H. H. Coenen, and S. M. Qaim, Appl. Radiat. Isot. **68**, 2001 (2010).
[41] M. S. Uddin, S. Sudár, and S. M. Qaim, Phys. Rev. C **84**, 024605 (2011).
[42] V. Semkova, P. Reimer, T. Altzitzoglou, A. J. M. Plompen, C. Quétel, S. Sudár, J. Vogl, A. J. Koning, S. M. Qaim, and D. L. Smith, Phys. Rev. C **80**, 024610 (2009).
[43] T. von Egidy, A. N. Behkami, and H. H. Schmidt, Nucl. Phys. A **454**, 109 (1986); T. von Egidy, H. H. Schmidt, and A. N. Behkami, *ibid.* **481**, 189 (1988).
[44] T. von Egidy and D. Bucurescu, Phys. Rev. C **78**, 051301R (2008).
[45] T. von Egidy and D. Bucurescu, Phys. Rev. C **80**, 054310 (2009).
[46] S. I. Al-Quraishi, S. M. Grimes, T. N. Massey, and D. A. Resler, Phys. Rev. C **67**, 015803 (2003).
[47] A. J. Koning, S. Hilaire, and S. Goriely, Nucl. Phys. A **810**, 13 (2008).
[48] R. Capote *et al.*, Nucl. Data Sheets **110**, 3107 (2009); [http://www-nds.iaea.org/RIPL-3/].

[49] M. B. Chadwick and P. G. Young, Nucl. Sci. Eng. **108**, 117 (1991).
[50] M. B. Chadwick, P. G. Young, P. Oblozinsky, and A. Marcinkowski, Phys. Rev. C **49**, R2885 (1994).
[51] M. B. Chadwick, A. V. Ignatyuk, A. B. Pashchenko, H. Vonach, and P. G. Young, Fusion Eng. Des. **37**, 79 (1997).
[52] H. Feshbach, A. Kerman, and S. Koonin, Ann. Phys. (NY) **125**, 429 (1980).
[53] C. Y. Fu, Nucl. Sci. Eng. **92**, 440 (1986).
[54] Ye. A. Bogila, V. M. Kolomietz, A. I. Sanzhur, and S. Shlomo, Phys. Rev. Lett. **75**, 2284 (1995).
[55] T. Kawano, P. Talou, and M. B. Chadwick, Nucl. Instrum. Methods Phys. Res. Sect. A **562**, 774 (2006).
[56] D. Dashdorj *et al.*, Phys. Rev. C **75**, 054612 (2007).
[57] N. Fotiades, R. O. Nelson, M. Devlin, S. Holloway, T. Kawano, P. Talou, M. B. Chadwick, J. A. Becker, and P. E. Garrett, Phys. Rev. C **80**, 044612 (2009).
[58] N. Patronis, C. T. Papadopoulos, S. Galanopoulos, M. Kokkoris, G. Perdikakis, R. Vlastou, A. Lagoyannis, and S. Harissopulos, Phys. Rev. C **75**, 034607 (2007).
[59] A. Tsinganis, M. Diakaki, M. Kokkoris, A. Lagoyannis, E. Mara, C. T. Papadopoulos, and R. Vlastou, Phys. Rev. C **83**, 024609 (2011).
[60] V. Avrigeanu, M. Avrigeanu, and F. L. Roman, EPJ Web Conf. **21**, 03001 (2012).
[61] M. Uhl and B. Strohmaier, Report IRK-76/01, IRK, Vienna, 1981.
[62] M. Avrigeanu and V. Avrigeanu, STAPRE-H95 Computer Code, IPNE Report NP-86-1995, Bucharest, 1995, and references therein; News NEA Data Bank **17**, 22 (1995).
[63] M. Blann, Nucl. Phys. A **213**, 570 (1973); M. Blann and H. K. Vonach, Phys. Rev. C **28**, 1475 (1983).
[64] M. Avrigeanu, M. Ivascu, and V. Avrigeanu, Z. Phys. A **329**, 177 (1988).
[65] M. Avrigeanu, M. Ivascu, and V. Avrigeanu, Z. Phys. A **335**, 299 (1990).
[66] L. Milazzo-Colli and G. M. Braga–Marcazzan, Nucl. Phys. A **210**, 297 (1973); E. Gadioli, E. Gadioli-Erba, and J. J. Hogan, Phys. Rev. C **16**, 1404 (1977).
[67] E. Gadioli and E. Gadioli-Erba, Z. Phys. A **299**, 1 (1981).
[68] M. Avrigeanu and V. Avrigeanu, J. Phys. G: Nucl. Part. Phys. **20**, 613 (1994).
[69] M. Avrigeanu and V. Avrigeanu, Comp. Phys. Comm. **112** (1998); A. Harangozo, I. Stetcu, M. Avrigeanu, and V. Avrigeanu, Phys. Rev. C **58**, 295 (1998).
[70] A. J. Koning and J. P. Delaroche, Nucl. Phys. A **713**, 231 (2003).
[71] K. Wisshak, F. Voss, F. Käppeler, M. Krtička, S. Raman, A. Mengoni, and R. Gallino, Phys. Rev. C **73**, 015802 (2006).
[72] A. J. Koning, S. Hilaire, and M. C. Duijvestijn, TALYS-1.0, in *Proceedings of the International Conference on Nuclear Data for Science and Technology, Nice, 2007*, edited by O. Bersillon *et al.* (EDP Sciences, Paris, 2008), p. 211; version TALYS-1.2, December 2009; [http://www.talys.eu/home/].
[73] V. Avrigeanu, P. E. Hodgson, and M. Avrigeanu, Phys. Rev. C **49**, 2136 (1994).
[74] M. Avrigeanu, W. von Oertzen, and V. Avrigeanu, Nucl. Phys. A **764**, 246 (2006).
[75] D. G. Gardner and F. S. Dietrich, Report UCRL-82998, LLNL-Livermore, 1979.
[76] M. Avrigeanu, V. Avrigeanu, G. Cata, and M. Ivascu, Rev. Roum. Phys. **32**, 837 (1987).
[77] S. Joly, Nucl. Sci. Eng. **94**, 94 (1986).
[78] J. Kopecky and M. Uhl, Phys. Rev. C **41**, 1941 (1990).
[79] C. H. Johnson, Phys. Rev. C **16**, 2238 (1977).
[80] H. Vonach, M. Uhl, B. Strohmaier, B. W. Smith, E. G. Bilpuch, and G. E. Mitchell, Phys. Rev. C **38**, 2541 (1988).
[81] Evaluated Nuclear Structure Data File (ENSDF), [http://www.nndc.bnl.gov/ensdf/].
[82] A. V. Ignatyuk, G. N. Smirenkin, and A. S. Tishin, Yad. Fiz. **21**, 485 (1975); Sov. J. Nucl. Phys. **21**, 255 (1976).
[83] A. R. Junghans, M. de Jong, H.-G. Clerc, A. V. Ignatyuk, G. A. Kudyaev, and K.-H. Schmidt, Nucl. Phys. A **629**, 635 (1998).
[84] A. J. Koning and M. B. Chadwick, Phys. Rev. C **56**, 970 (1997).
[85] A. Bohr and B. R. Mottelson, *Nuclear Structure* (Benjamin, Inc., Advanced Book Program, Reading, 1969), p. 141.
[86] A. A. Filatenkov and S. V. Chuvaev, Khlopin Radium Institute Preprint KRI-259, CNIIatominform, Moscow, 2003.
[87] Experimental Nuclear Reaction Data (EXFOR), [www-nds.iaea.or.at/exfor].
[88] M. B. Chadwick *et al.*, Nucl. Data Sheets **107**, 2931 (2006).
[89] Balraj Singh, Nucl. Data Sheets **107**, 1531 (2006).
[90] M. A. Gardner and D. G. Gardner, Lawrence Livermore National Laboratory Report UCRL-92492, Livermore, 1985.
[91] M. Mirea (private communication).
[92] B. Pichon, Nucl. Phys. A **568**, 553 (1994).
[93] X. Ledoux *et al.*, in *11th International Conference on Applications of Nuclear Techniques Crete, Greece, June 12-18, 2011* (to be published); [http://pro.ganil-spiral2.eu/spiral2/instrumentation/nfs].
[94] E. Chiaveri *et al.* (The n_TOF Collaboration), EPJ Web Conf. **21**, 03001 (2012); [https://twiki.cern.ch/twiki/bin/view/NTOF/].